

Potential Hepatoprotective Effects of Irbesartan, an Accessible Angiotensin II Receptor Blocker, Against Cisplatin-Induced Liver Injury in a Rat Model

Short Title: Irbesartan and cisplatin-induced liver injury

Onur ERTUNÇ¹, Yalçın ERZURUMLU², Mehtap SAVRAN³, Deniz ÇATAKLI⁴,
Eltaf DOĞAN KIRAN⁵, Şakir PEKGÖZ⁶

¹Department of Pathology, Faculty of Medicine, Suleyman Demirel University, Isparta, Turkey

²Department of Biochemistry, Faculty of Pharmacy, Suleyman Demirel University, Isparta, Turkey

³Department of Pharmacology, Faculty of Medicine, Suleyman Demirel University, Isparta, Turkey

⁴Department of Pharmacology, Faculty of Medicine, Suleyman Demirel University, Isparta, Turkey

⁵Department of Biochemistry, Faculty of Medicine, Suleyman Demirel University, Isparta, Turkey

⁶Department of Pathology, Faculty of Medicine, Suleyman Demirel University, Isparta, Turkey

*Corresponding author

Onur ERTUNÇ

Department of Pathology, Faculty of Medicine, Suleyman Demirel University, Isparta, Turkey

e-mail: onurertunc@hotmail.com

Mobile: +905422206621

Fax: + 092462112830

ORCID: (<https://orcid.org/0000-0002-4159-1711>)

06.11.2022

06.05.2023

09.05.2023

Conflict of Interest

No conflict of interest was reported by the authors.

Financial Support

This study was supported by Scientific Research Fund of the Suleyman Demirel University (Project number: TSG-2020-8134).

ABSTRACT

Objectives: Drug-induced liver injury is a common adverse reaction that frequently occurs with chemotherapeutic agents, such as cisplatin (CIS). The present study seeks to enhance our comprehension of drug actions and their associated adverse effects by examining the toxicity of cisplatin on rat liver tissue. Basically, we aim to investigate the potential hepatoprotective effects of irbesartan (IRB), an easily accessible angiotensin II receptor blocker, in mitigating the hepatotoxicity induced by cisplatin.

Methods: Wistar albino rats were divided into four groups. These groups included a control group (saline, peroral [p.o.] for seven days, and 1 ml saline intraperitoneal [i.p.] on the fourth day); a CIS group (1 ml saline for seven days and 7.5 mg/kg CIS i.p. on the fourth day); a CIS+IRB group (IRB: 50 mg/kg p.o. for seven days and 7.5 mg/kg CIS i.p. on the fourth day); an IRB group (50mg/kg IRB p.o. for seven days). The effect of Irbesartan on IL-1 beta (IL-1 β) and Caspase 3 levels was evaluated by immunohistochemical analysis, and its effects on mRNA expression levels of CCAAT/enhancer-binding protein (C/EBP) homologous protein (CHOP) and Immunoglobulin-heavy-chain-binding protein (BiP) were tested by quantitative real-time polymerase chain reaction (qRT-PCR).

Results: The administration of irbesartan mitigated cisplatin-induced liver toxicity by inhibiting endoplasmic reticulum (ER) stress. Specifically, this drug reduced the mRNA expression of ER stress markers, including CHOP and BiP. In addition, irbesartan treatment decreased oxidative stress, inflammatory responses, and apoptotic markers.

Conclusion: These findings suggest that irbesartan may be a promising therapeutic option for preventing cisplatin-induced liver injury, potentially by modulating ER stress-related pathways.

Keywords: Cisplatin, ER-stress, Irbesartan, Liver toxicity.

INTRODUCTION

CIS (cis-diamminedichloroplatinum) is one of the most commonly preferred chemotherapeutic agents in the treatment of malignancies. Several adverse effects can be seen by the CIS treatment, such as nephrotoxicity, GI disorders, neurotoxicity, ototoxicity, hepatotoxicity, and cardiotoxicity.^{1,2} CIS-induced hepatotoxicity is the most frequently faced adverse effect that reduces therapeutic efficacy and limits the usage of this drug in cancer therapy.³ Studies showed that CIS-induced toxicity might result from mitochondrial dysfunction, excessive reactive oxygen species (ROS) production, increased tumor necrosis factor-alpha (TNF- α) levels, and induction of endoplasmic reticulum (ER) stress. Although there are predictable links between ER stress and anticancer drug-induced liver injury, the underlying mechanism remains unclear.^{4,5}

The ER is a multifunctional organelle found in eukaryotic cells and consists of sac-like structures and branched tubules. It has regulated numerous pivotal functions, including protein biosynthesis, folding, trafficking, and calcium storage, as well as lipogenesis.^{6,7} Altering physiological conditions affect ER homeostasis for various reasons, such as genetic mutations, heat shock, oxidative stress, or multiple pathophysiologies. Furthermore, increased protein synthesis requirement, glucose deprivation, or imbalance in ER calcium stock levels can cause impaired functionality of ER, termed ER stress.⁸

The unfolded protein response (UPR) signaling is responsible for re-establishing cellular homeostasis against ER stress, and it is regulated with ER-membrane localized three transmembrane proteins: Inositol-requiring kinase 1 alpha (IRE1 α), Protein kinase R-like endoplasmic reticulum kinase (PERK) and activating transcription factor 6 (ATF6). Also, it coordinates the ER protein folding capacity, proteostasis, and programmed cell death under prolonged UPR activation. Additionally, UPR has been associated with acquiring drug resistance in numerous pathologies.^{7,9}

Protein aggregation in the ER lumen or insufficient ER capacity causes the releasing glucose-regulated protein 78 (GRP78), also regarded as Immunoglobulin-heavy-chain-binding protein (BiP), from the UPR sensors to which it is attached. BiP is a member of the heat shock protein family and is a key player that manages ER stress responses.¹⁰ Thus, BiP levels in the ER pool have a critical role in managing ER stress. Furthermore, PR regulates the expression level of

various cell death-associated inducers, such as C/EBP homologous protein (CHOP), also known as GADD153.¹⁰ CHOP is a pro-apoptotic transcription factor induced by ER stress and mediates apoptosis.¹² Because of these critical roles of BiP and CHOP proteins, changes in their levels are frequently evaluated in investigating ER stress at the cellular level.

Metabolic dysregulation induced by excessive amounts of lipids, glucose, cytokines, neurotransmitters, or exposure to chemotherapeutic agents, leads to ER stress. This disruption in normal cellular function can contribute to the exacerbation of inflammatory responses and other associated pathologies.¹³ Recent studies suggest that ER stress management is a potent target for new therapeutic approaches to be developed against cancer or tissue injuries.^{14,15}

IRB is an angiotensin II receptor blocker that is commonly used in the treatment of hypertension. IRB acts on the renin-angiotensin system and shows protective effects on diverse organs in the body, such as the heart, kidney, and liver. Besides, IRB is known to have anti-inflammatory, antioxidant, and antifibrotic effects.¹⁶ Emerging research has demonstrated that various pharmaceutical agents used in cancer treatment can induce a robust ER stress response. This novel insight may offer new avenues for developing more effective therapeutic strategies.^{17,18} Also, the efficacy of drug or chemoresistance occurrence can be alleviated by modulation of ER stress. This approach can be an important factor that could alter the treatment of adverse responses.¹⁸ However, today, the relationship between ER stress and the action of anticancer drugs remains unclear. Herein, we aimed to shed light on the potential protective mechanisms underlying IRB against CIS-induced hepatotoxicity. To achieve this, we evaluated the impact of IRB on ER stress, oxidative stress parameters, and the expression levels of anti-inflammatory cytokines. Present findings may offer valuable insights into IRB's therapeutic potential in managing drug-induced liver injury.

METHODS

Animals

Adult male Wistar albino rats (n=32) with an average weight of 250-300g were obtained from the Animal Research Laboratory. They were group-housed (eight rats per cage) under a 12/12 h light/dark cycle at room temperature (24 ± 1 °C) with a relative humidity of $50 \pm 10\%$ with access to food and water ad libitum. Animals were acclimatized for at least seven days before experimentation (Figure 1). All experimental procedures were permitted by the National Institutes

of Health and Committee on Animal Research according to the ethical rules (Protocol number: 23.09.2021 09/03).

All rats were randomly separated into four groups as follows:

- 1) The control group was given 1ml saline per oral (p.o.) for seven days. On the fourth day, 1 ml saline was given intraperitoneal (i.p.).
- 2) The CIS group was administered 1ml saline p.o. for seven days, and 7.5 mg/kg i.p. CIS (Cisplatin, Koçak Farma, Turkey) was implemented on the fourth day.¹⁹
- 3) The CIS + IRB group was given 50 mg/kg IRB (Sandoz, Switzerland) p.o. for seven days, and 7.5mg/kg CIS i.p. was administered on the fourth day.²⁰
- 4) The IRB group was administered 50 mg/kg IRB p.o. for seven days, and 1 ml saline i.p. was implemented on the fourth day.

The sacrifice of animals was carried out 6 h after following the last drug administration under ketamine (80–100 mg/kg) (Alfamin, Alfasan IBV) and 8–10 mg/kg xylazine bio 2% solution (Bioveta, Czech Republic) anesthesia. Liver tissues were then removed. One part of the tissues was converged for total antioxidant status (TAS), total oxidant status (TOS), and immunoblotting assay. The remaining part of the tissue was fixed in 10% buffered formaldehyde for histopathological examination and immunohistochemical analysis.

Histopathological analysis

The liver was removed and fixed in 10% buffered formalin during the necropsy and taken for routine pathology processing after macroscopic sampling by an automatic tissue processor (Leica ASP300S, Wetzlar, Germany) and embedded in a paraffin block. 5 µ(micron) thick sections were taken from blocks by microtome (Leica RM2155, Leica Microsystems, Wetzlar, Germany). Then, hematoxylin-eosin (HE) staining was used to stain sections and monitored by a light microscope.

Immunohistochemical analysis

Two sections were taken from all groups of the liver samples and put in poly-L-lysine coated slides. Then, immunohistochemical staining of slices with anti-caspase-3 (sc-7272, 1:100, Santa Cruz (Texas, USA) and anti-IL-1β (sc-52012, 1:100 dilution, Santa Cruz (Texas, USA)) was carried out by streptavidin-biotin technique consistent with manufacturer's protocol. The incubation of sections with primary antibodies for 60 min was performed, then immunohistochemistry using biotinylated secondary antibody and streptavidin-alkaline phosphate conjugate was carried out. The secondary antibodies of EXPOSE Mouse and Rabbit Specific

HRP/DAB Detection IHC kit (ab80436) (Abcam, Cambridge, UK) were used. Diaminobenzidine (DAB) was used as the chromogen. Antigen dilution solution was used as a negative control. Blinding was done in the examination of samples. Semiquantitative analysis was performed to quantify the intensity of the immunohistochemical markers using a grading score ranging from (0) to (3) as follows: (0) = negative, (1) = weak focal staining, and $\leq 10\%$, (2) = diffuse weak staining and $\geq 10\%$, (3) = intense diffuse staining and $\geq 10\%$.²¹ Independent ten different areas of each section were analyzed under 40X objective magnification by an experienced pathologist. Database Manual Cell Sens Life Science Imaging Software System (Olympus Co., Tokyo, Japan) was used for morphometric analyses and microphotography.

Quantitative real-time polymerase chain reaction (qRT-PCR)

Total RNA was extracted from rat tissues by column type miniprep kit (Bio-Rad, Hercules, CA, USA) following the manufacturer's protocol. Then, complementary DNA was synthesized with a cDNA Synthesis kit (Bio-Rad Laboratories, Hercules, CA). The cDNA was amplified using the iTaQ Universal SYBR Green Supermix in a CFX96 instrument (Bio-Rad Laboratories, Hercules, CA). In PCR processes, pre-denaturation at 95 °C for 10 minutes, followed by 40 cycles at 95 °C for 10 seconds, and at 60 °C for 30 seconds were followed. Melting-curve analysis was performed to confirm the specificity of PCR amplicons. Specific primers were designed to amplify BiP (Forward 5'-TGT GAC TGT ACC AGC TTA CTT C-3', Reverse 5'-TCT TCT CTC CCT CTC TCT TAT CC-3'), CHOP (Forward 5'- GGA GGC TAC ACT CTA CAA AGA AC-3', Reverse 5'-CCT TCT AAC GCT TCC CAA AGA-3'), GAPDH (Forward 5'-CAA GGT CAT CCC AGA GCT GAA-3', Reverse 5'-CAT GTA GGC CAT GAG GTC CAC-3'). The housekeeping gene GAPDH was used to normalize relative gene expression. Relative mRNA expression levels were analyzed by using the Livak method.²²

Detection of Oxidative Stress Markers

Biochemical analyses included measurements of TAS, TOS, and OSI levels. For oxidant-antioxidant analysis, liver tissue samples were homogenized. The spectrophotometric measurement of the total antioxidant status (TAS) and total oxidant status (TOS) was performed by using commercial kits consistent with the manufacturer's instruction (Rel Assay Diagnostics, Gaziantep, Turkey), and TOS/TAS ratio was noticed as OSI value.^{23,24}

Liver function parameters measurement

The serum samples were obtained from the blood of rats by centrifugation at 3000 rpm for 10 minutes. The levels of aspartate transaminase (AST) and alanine aminotransferase (ALT) in serum were determined using the spectrophotometric technique on an autoanalyzer (Beckman Coulter, USA) with the instrument's kit.

Statistical Analysis

Statistical analysis was performed using GraphPad Prism 5 (San Diego, California, USA) software. Results were expressed as mean \pm SD. One-way ANOVA followed by Bonferroni, multiple comparison test, was used to compare the groups. $p < 0.05$ were considered significant.

RESULTS

Histopathological finding

In hematoxylin-eosin staining, ten fields at 40x magnification were evaluated in the same way immunohistochemical expressions were assessed. The liver is typically organized into hexagonal lobules containing the central vein at the center and the portal vein, hepatic artery, and bile duct at the corners. Hepatic sinusoids connect the central vein to the portal vein (as depicted in Figure 2E). Following four days of cisplatin treatment, rats exhibited liver congestion, increased Kupffer cells, and reactive changes such as nucleolar prominence, as observed in liver sections (Figure 2A, 2B). However, in the group treated with both CIS and IRB, congestion in the hepatic sinus was reduced, as demonstrated by H&E slides (Figure 2C). Interestingly, in the IRB-treated group, there was an increase in cytoplasmic eosinophilia (Figure 2D).

Immunohistochemical findings

Immunohistochemical (IHC) evaluation showed that CIS administration caused a significant increase in caspase 3 and IL-1 β expressions in the liver tissues of rats ($p < 0.001$). IRB treatment reversed CIS-induced increment in caspase 3 and IL-1 β expressions ($p < 0.01$, $p < 0.001$, respectively) (Figure 3,4).

qRT-PCR Results

Elevated mRNA expression level of CHOP and BiP was detected in the CIS group compared to the control. ($p < 0.05$, $p < 0.001$; respectively). The combined treatment of CIS and IRB significantly decreased the expression level of CHOP and BiP compared to the CIS group ($p < 0.01$). Only IRB treatment significantly reduced CHOP and BiP levels compared with the CIS group ($p < 0.001$, $p < 0.01$, respectively) (Figure 5).

Biochemical Results

Oxidative Stress Parameters

A significant decrement in TAS levels was determined in the CIS group compared to the control. ($p < 0.01$, Figure 6). In the CIS +IRB and IRB groups, TAS levels increased compared to the CIS group ($p < 0.001$ for both). OSI levels elevated in the CIS group compared to the control group ($p < 0.01$). In the CIS+IRB group, OSI level attenuated compared to the CIS group ($p < 0.01$) (Figure 6).

Liver Function Parameters

The ALT and AST levels of the CIS group were significantly higher than the control ($p < 0.001$, $p < 0.01$, respectively). In the CIS+IRB group, ALT and AST levels attenuated compared to the CIS group ($p < 0.001$, $p < 0.01$, respectively). Contrary to this, ALT level attenuated in the IRB group compared to the CIS+IRB group ($p < 0.05$) (Figure 7).

DISCUSSION

IRB is a commonly used angiotensin-converting enzyme-II blocker and is effective in treating hypertension related cardiovascular diseases.²⁵ It is also known that the renin-angiotensin system (RAS) plays a pivotal role in the physiological system, especially in blood pressure regulation and its components including angiotensin II, which is highly expressed in various tissues, such as the kidney, adipose, and liver.²⁶⁻²⁸ Moreover, inhibition of RAS by ACE inhibitors or either angiotensin receptor antagonists presented as a therapeutic approach for liver fibrosis.²⁹ It has been shown that the effects of these drugs are not limited to angiotensin blockage, but they also have ameliorative activity on oxidative stress, glutathione depletion, and lipid peroxidation.³⁰⁻³² *In vivo* and *in vitro* studies performed on cardiomyocytes have shown that angiotensin II induces ER stress.³³ The study conducted on human pancreatic islet cells demonstrated a protective effect of Losartan which is another ACE inhibitor, against glucose-induced ER stress responses.³⁴ Although detailed examines of the anti-inflammatory and antioxidant effects of IRB in various studies, the other hand, ER stress-related outcomes of IRB still need to be clearly understood.²⁵ A.M. Kabel *et al.* demonstrated that IRB exhibited hepatoprotective effects by inhibiting apoptosis in hepatic tissues.¹⁶ Thus, we aimed to investigate the IRB's underlying mechanism in CIS-induced hepatotoxicity by evaluating ER stress-related responses.

CIS is a chemotherapeutic drug that shows efficiency against various cancer types like testicular, gastric, ovarian, lung, and breast.⁴ However, almost 30% of patients may face the adverse effects of CIS, which limits drug usage in therapy.³ There are numerous side effects of CIS, but hepatotoxicity is still at the top. So far, proven mechanisms of CIS-induced hepatotoxicity are mitochondrial dysfunction, oxidative stress, inflammation apoptosis, and disrupted Ca^{+2} homeostasis.³⁵

Recent studies have shown that possible ER stress-mediated mechanisms may have a critical role in hepatotoxicity progression.³⁶ ER membrane-localized sensor proteins (IRE1 α , PERK, and ATF6) fine-tune the ER stress responses for the cells to adapt to changing physiological conditions.¹¹ Particularly, releasing BiP protein from ER-stress sensors leads to the activation of UPR signaling. When the cells cannot overcome the prolonged ER stress, the expression levels of CHOP increase, which is a downstream effector of the PERK branch of UPR, and programmed cell death is triggered through CHOP-controlled apoptotic proteins.³⁷ Thus, cells' survival or programmed-cell death decision is made under ER stress. Herein, we evaluated mRNA expression levels of CHOP, a pro-apoptotic factor, and its high expression levels lead cells to mediate programmed cell death. Also, we tested the mRNA expression levels of BiP, which is an ER chaperone and is frequently used as a marker to monitor ER stress.³⁸

In studies where we investigated the protective effects of IRB against CIS-induced hepatotoxicity, our findings indicated that IRB administration significantly restores CIS-induced tissue damage by decreasing ER stress induction (Fig. 6). We determined that IRB significantly reduced the CIS-induced mRNA expression levels of BiP and CHOP. These results suggest that IRB has a protective role in CIS-induced hepatotoxicity by reducing the CIS-mediated elevating BiP and CHOP levels.

CHOP protein is also associated with one of the mechanisms that lead to ROS production linked to ER stress.³⁹ For that reason, to more detailed understand the protective role of IRB against CIS-induced tissue damage, we evaluated the TAS, TOS, and OSI levels. As expected, CIS treatment caused a decrement in the TAS level and an increment in the OSI level (Fig. 7).

The feedback between inflammatory cell responses and ER-stress response might trigger apoptosis in several pathological conditions.⁴⁰ ER stress may lead to activation of NF- κ B (nuclear factor kappa-light-chain-enhancer of activated B cells) phosphorylation and increment in the proinflammatory and apoptotic cytokines synthesis and release from the cell, contributing to the

inflammatory and apoptotic cycle progression.⁴¹ As known, IL-1 β and Cas-3 are common inflammatory and apoptotic mediators, respectively. Also, they are cross-talking to each other through the NF- κ B pathway.⁴² Previous studies indicate that IRB could prevent inflammation by inhibiting the NF- κ B pathway.²⁵

Our findings suggested that CIS administration strongly increased CHOP and BiP mRNA expressions, resulting in increased IL-1 and Cas-3 levels; contrarily, IRB administration significantly decreased IL-1 and Cas-3 levels, as seen in the results of immunohistochemistry. Also, present histopathologic findings overlapped with the literature.^{25,43} Consistent with immune staining results, our histological findings supported the protective role of IRB on CIS-induced liver tissue damage. In the CIS group, sinusoidal dilatation and apoptotic bodies increased compared to the normal group. Apart from that, we detected a significant increase in eosinophilic cytoplasm in the IRB+CIS and IRB groups, which might result from cellular hypertrophy or peroxisomal and smooth endoplasmic reticulum or mitochondrial enhanced activity in the liver cell. Collectively these results suggest that IRB effectively reverses CIS-induced hepatocellular tissue damage by decreasing ER stress and inflammatory responses triggered by CIS administration.

Moreover, we measured the impact of IRB on hepatic tissues related biochemical parameters. ALT and AST are regarded as serological markers of pathologies in liver tissue. Biochemical detection of ALT is especially susceptible to detecting liver injury.⁴⁴ Also, AST is found in the mitochondria of hepatocytes, and when injury of hepatocytes occurs, it is released into the blood.⁴⁵ Our results showed that CIS administration elevated the level of ALT and AST (Fig. 8). These results suggested that IRB significantly reversed CIS-induced liver injury and inflammation in hepatocellular tissue. Also, consistent with the literature, our findings indicate that IRB might protect the hepatocellular tissue against CIS-induced tissue damage by regulating ER stress and oxidative stress status.

Main Points

- Irbesartan reverses cisplatin-induced oxidative stress.
- Irbesartan modulates cisplatin-induced liver dysfunction by reorganizing the main liver enzymes.
- Irbesartan reduces cisplatin-induced ER stress.

Study Limitations

The present study just tested the effects of IRB on mRNA levels of CHOP and BiP. Therefore, further detailed analyses are required for a better understanding of the effect of IRB on ER stress modulation and the protective roles against CIS-induced liver injury.

CONCLUSION

Herewith, we aimed to investigate the possible effects of IRB on CIS-induced hepatotoxicity. Our findings suggest that IRB may have some protective roles against CIS-induced liver toxicity. But, further studies are needed to elucidate the mode of action of IRB in liver toxicity.

References

1. Lee HY, Mohammed KA, Goldberg EP, Kaye F, Nasreen N. Cisplatin loaded albumin mesospheres for lung cancer treatment. *Am J Cancer Res*. 2015;5:603–15.
2. Breglio AM, Rusheen AE, Shide ED, Fernandez KA, Spielbauer KK, McLachlin KM, et al. Cisplatin is retained in the cochlea indefinitely following chemotherapy. *Nat Commun*. 2017;8:1654.
3. Lebwohl D, Canetta R. Clinical development of platinum complexes in cancer therapy: an historical perspective and an update. *Eur J Cancer*. 1998;34:1522–34.
4. Dasari S, Tchounwou PB. Cisplatin in cancer therapy: molecular mechanisms of action. *Eur J Pharmacol*. 2014;740:364–78.
5. Foufelle F, Fromenty B. Role of endoplasmic reticulum stress in drug-induced toxicity. *Pharmacol Res Perspect*. 2016;4:e00211.
6. Berridge MJ. The endoplasmic reticulum: a multifunctional signaling organelle. *Cell Calcium*. 2002;32:235–49.
7. Hetz C. The unfolded protein response: controlling cell fate decisions under ER stress and beyond. *Nat Rev Mol Cell Biol*. 2012;13:89–102.
8. Li A, Song NJ, Riesenberger BP, Li Z. The Emerging Roles of Endoplasmic Reticulum Stress in Balancing Immunity and Tolerance in Health and Diseases: Mechanisms and Opportunities. *Front Immunol*. 2019;10:3154.
9. Storm M, Sheng X, Arnoldussen YJ, Saatcioglu F. Prostate cancer and the unfolded protein response. *Oncotarget*. 2016;7:54051–66.

10. Wang M, Wey S, Zhang Y, Ye R, Lee AS. Role of the unfolded protein response regulator GRP78/BiP in development, cancer, and neurological disorders. *Antioxid Redox Signal*. 2009 ;11:2307–2316.
11. Bertolotti A, Zhang Y, Hendershot LM, Harding HP, Ron D. Dynamic interaction of BiP and ER stress transducers in the unfolded-protein response. *Nat Cell Biol*. 2000;2:326–332.
12. Oyadomari S, Mori M. Roles of CHOP/GADD153 in endoplasmic reticulum stress. *Cell Death Differ*. 2004;11:381–9.
13. Lin YD, Chen S, Yue P, Zou W, Benbrook DM, Liu S, et al. CAAT/Enhancer Binding Protein Homologous Protein–Dependent Death Receptor 5 Induction Is a Major Component of SHetA2-Induced Apoptosis in Lung Cancer Cells. *Cancer Research*. 2008; 68:5335–5344.
14. Erzurumlu Y, Dogan HK, Catakli D, Aydogdu E. Tarantula cubensis Extract Induces Cell Death in Prostate Cancer by Promoting Autophagic Flux/ER Stress Responses and Decreased Epithelial-Mesenchymal Transition. *Revista Brasileira de Farmacognosia*. 2022;32: 575-582.
15. Ashrafizadeh M, Tavakol S, Ahmadi Z, Roomiani S, Mohammadinejad R, Samarghandian S. Therapeutic effects of kaempferol affecting autophagy and endoplasmic reticulum stress. *Phytother Res*. 2020;34:911–23.
16. Kabel AM, Alzahrani AA, Bawazir NM, Khawtani RO, Arab HH. Targeting the proinflammatory cytokines, oxidative stress, apoptosis and TGF- β 1/STAT-3 signaling by irbesartan to ameliorate doxorubicin-induced hepatotoxicity. *J Infect Chemother*. 2018 ;24:623–31.
17. Jeon YJ, Khelifa S, Ratnikov B, Scott DA, Feng Y, Parisi F, et al. Regulation of glutamine carrier proteins by RNF5 determines breast cancer response to ER stress-inducing chemotherapies. *Cancer Cell*. 2015;27:354–69.
18. Cubillos-Ruiz JR, Bettigole SE, Glimcher LH. Tumorigenic and Immunosuppressive Effects of Endoplasmic Reticulum Stress in Cancer. *Cell*. 2017;168:692–706.

19. Alibakhshi T, Khodayar MJ, Khorsandi L, Rashno M, Zeidooni L. Protective effects of zingerone on oxidative stress and inflammation in cisplatin-induced rat nephrotoxicity. *Biomed Pharmacother.* 2018;105:225–32.
20. Anjaneyulu M, Chopra K. Effect of irbesartan on the antioxidant defence system and nitric oxide release in diabetic rat kidney. *Am J Nephrol.* 2004;24:488–96.
21. Calhoun BC, Collins LC. Predictive markers in breast cancer: An update on ER and HER2 testing and reporting. *Semin Diagn Pathol.* 2015;32:362–9.
22. Livak KJ, Schmittgen TD. Analysis of relative gene expression data using real-time quantitative PCR and the 2(-Delta Delta C(T)) Method. *Methods.* 2001;25:402–8.
23. Erel O. A novel automated direct measurement method for total antioxidant capacity using a new generation, more stable ABTS radical cation. *Clin Biochem.* 2004;37:277–85.
24. Erel O. A new automated colorimetric method for measuring total oxidant status. *Clin Biochem.* 2005;38:1103–11.
25. Helal MG, Samra YA. Irbesartan mitigates acute liver injury, oxidative stress, and apoptosis induced by acetaminophen in mice. *J Biochem Mol Toxicol.* 2020;34:e22447.
26. Yvan-Charvet L, Quignard-Boulangé A. Role of adipose tissue renin-angiotensin system in metabolic and inflammatory diseases associated with obesity. *Kidney Int.* 2011;79:162–8.
27. Kalupahana NS, Moustaid-Moussa N. The renin-angiotensin system: a link between obesity, inflammation and insulin resistance. *Obes Rev.* 2012;13:136–49.
28. Ramalingam L, Menikdiwela K, LeMieux M, Dufour JM, Kaur G, Kalupahana N, et al. The renin angiotensin system, oxidative stress and mitochondrial function in obesity and insulin resistance. *Biochim Biophys Acta Mol Basis Dis.* 2017;1863:1106–14.
29. Bataller R, Brenner DA. Liver fibrosis. *The Journal of clinical investigation.* 2005;115:209-218.
30. Khaper N, Singal PK. Modulation of oxidative stress by a selective inhibition of angiotensin II type 1 receptors in MI rats. *J Am Coll Cardiol.* 2001;37:1461–6.

31. Jahovic N, Ercan F, Gedik N, Yüksel M, Sener G, Alican I. The effect of angiotensin-converting enzyme inhibitors on experimental colitis in rats. *Regul Pept.* 2005;130:67–74.
32. Kedziora-Kornatowska K. Effect of angiotensin convertase inhibitors and AT1 angiotensin receptor antagonists on the development of oxidative stress in the kidney of diabetic rats. *Clin Chim Acta.* 1999;287:19–27.
33. Yang C, Wang Y, Liu H, Li N, Sun Y, Liu Z, et al. Ghrelin protects H9c2 cardiomyocytes from angiotensin II-induced apoptosis through the endoplasmic reticulum stress pathway. *J Cardiovasc Pharmacol.* 2012;59:465–71.
34. Madec AM, Cassel R, Dubois S, Ducreux S, Vial G, Chauvin MA, et al. Losartan, an angiotensin II type 1 receptor blocker, protects human islets from glucotoxicity through the phospholipase C pathway. *FASEB J.* 2013;27:5122–30.
35. Ezz-Din D, Gabry MS, Farrag ARH, Moneim AEA. Physiological and histological impact of *Azadirachta indica* (neem) leaves extract in a rat model of cisplatin-induced hepato and nephrotoxicity. *Journal of Medicinal Plants Research.* 2011;5:5499–506.
36. Pandey VK, Mathur A, Khan MF, Kakkar P. Activation of PERK-eIF2 α -ATF4 pathway contributes to diabetic hepatotoxicity: Attenuation of ER stress by Morin. *Cell Signal.* 2019;59:41–52.
37. Ohoka N, Yoshii S, Hattori T, Onozaki K, Hayashi H. TRB3, a novel ER stress-inducible gene, is induced via ATF4-CHOP pathway and is involved in cell death. *The EMBO Journal.* 2005;24:1243–55.
38. Pobre KFR, Poet GJ, Hendershot LM. The endoplasmic reticulum (ER) chaperone BiP is a master regulator of ER functions: Getting by with a little help from ERdj friends. *J Biol Chem.* 2019;294:2098–108.
39. Zhang K, Kaufman RJ. From endoplasmic-reticulum stress to the inflammatory response. *Nature.* 2008;454:455–62.

40. Zeeshan HMA, Lee GH, Kim HR, Chae HJ. Endoplasmic Reticulum Stress and Associated ROS. *Int J Mol Sci.* 2016;17:327.
41. Baeuerle PA, Baichwal VR. NF- κ B as a frequent target for immunosuppressive and anti-inflammatory molecules. *Adv Immunol.* 1997;65:111–38.
42. Lamkanfi M, Declercq W, Vanden Berghe T, Vandenabeele P. Caspases leave the beaten track: caspase-mediated activation of NF- κ B. *J Cell Biol.* 2006;173:165–71.
43. Taghizadeh F, Hosseinimehr SJ, Zargari M, Karimpour Malekshah A, Mirzaei M, Talebpour Amiri F. Alleviation of cisplatin-induced hepatotoxicity by gliclazide: Involvement of oxidative stress and caspase-3 activity. *Pharmacol Res Perspect.* 2021;9:e00788.
44. Heydrnejad MS, Samani RJ, Aghaeivanda S. Toxic Effects of Silver Nanoparticles on Liver and Some Hematological Parameters in Male and Female Mice (*Mus musculus*). *Biol Trace Elem Res.* 2015;165:153–8.
45. Ennulat D, Magid-Slav M, Rehm S, Tatsuoka KS. Diagnostic performance of traditional hepatobiliary biomarkers of drug-induced liver injury in the rat. *Toxicol Sci.* 2010;116:397–412.

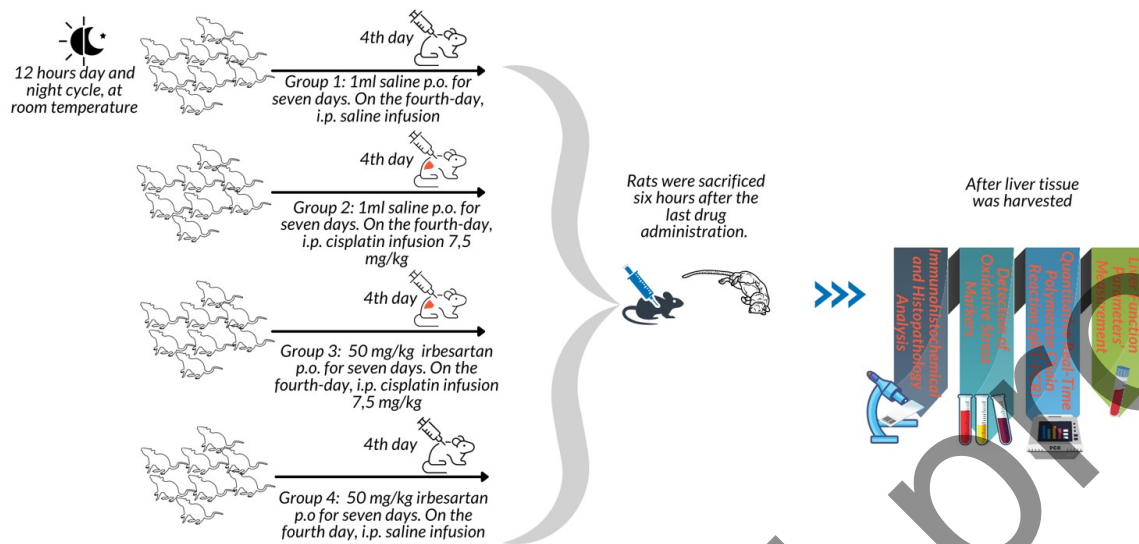


Figure 1: Experimental Procedures are depicted as in the drawing.

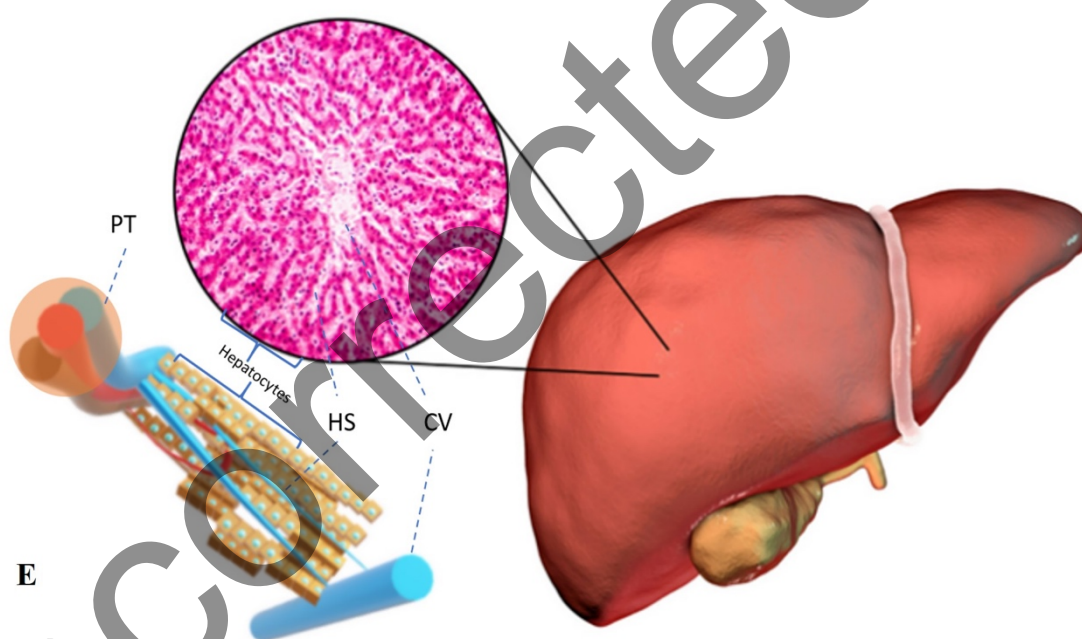
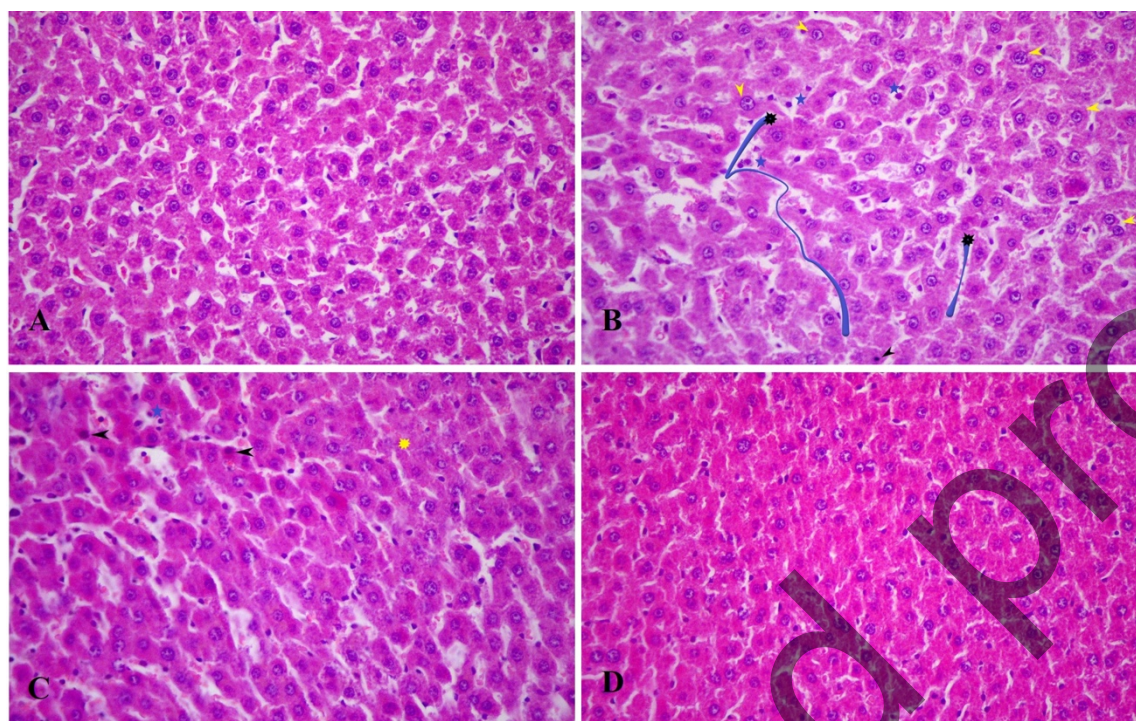


Figure 2: Histopathological findings in liver tissues. Normal parenchymal hepatocyte in control mouse (A), CIS-treated group; Sinusoidal spacing (shown in 3D line), sinusoidal Kupffer cells (blue star), reactive cellular alterations and nucleolar prominence (yellow arrows), and occasional apoptosis (black arrows) (B), CIS +IRB group; congestion, and sinusoidal spaces, increased eosinophilic cytoplasm (yellow mark), and sinusoidal Kupffer cells (blue star) and sporadic

apoptotic hepatocytes (black arrow) (C), IRB group; eosinophilic cytoplasm (D), hepatic lobules schema (E) (All H&E slides were captured by the microscope Nikon Ni-U at 200x magnification) (HS: hepatic sinus, CV: central vein, PT: portal triad).

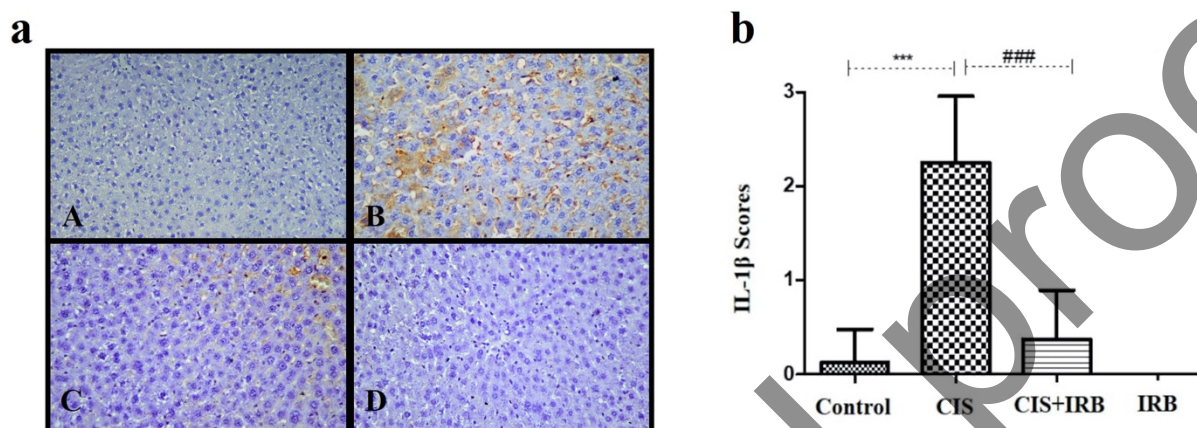


Figure 3: a) Immunohistochemical evaluation of IL-1 β levels. Negative expression in the control group (A), marked increase expression of CIS group (B), decreased expression of CIS+IRB group (C), lack expression in IRB group (D). b) Statistical analysis of IL-1 β levels. In the CIS group IL-1 β scores were found significantly higher than the control group ($p < 0.001$). In the CIS+IRB group, IL-1 β scores significantly decreased compared to the CIS group ($p < 0.001$). In the IRB group, IL-1 β scores were found significantly lower than the CIS group ($p < 0.001$). Comparison between groups was assessed by one-way ANOVA test followed by post hoc Bonferroni multiple comparison test.

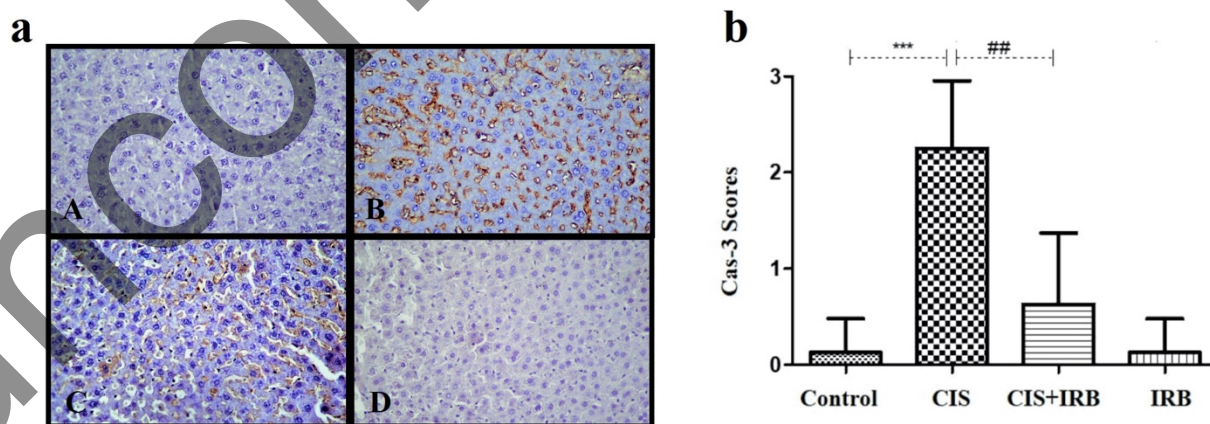


Figure 4: a) Immunohistochemical evaluation of caspase-3 levels. Negative expression in the control group (A), marked increase expression of CIS group (B), decreased expression of CIS+IRB

group (C), lack expression in IRB group (D) b) Statistical analysis of caspase-3 levels. In the CIS group caspase-3 scores were found significantly higher than the control group ($p<0.001$). In the CIS+IRB group, caspase-3 scores significantly decreased compared to the CIS group ($p<0.01$). Comparison between groups was assessed by one-way ANOVA test followed by post hoc Bonferroni multiple comparison test.

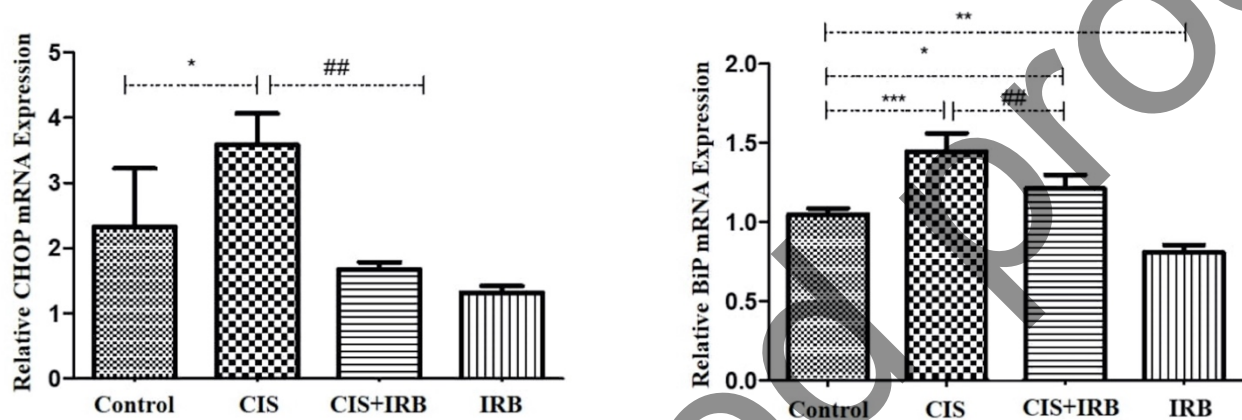


Figure 5: Evaluation of relative mRNA expression level of CHOP and BiP. mRNA expression levels of the CHOP and BiP were analyzed by qRT-PCR. Relative mRNA expression values were calculated using $2^{-\Delta\Delta CT}$ and GAPDH was used as a housekeeping Data represent the mean of four independent biological replicates in triplicates, and error bars represent SD. Comparison between groups was assessed by one-way ANOVA test followed by post hoc Bonferroni multiple comparison test. Values are represented as means \pm SD. ($n=3$) *** $p<0.001$ ** $p<0.01$ * $p<0.05$, '*' represents comparison with control group, ### $p<0.001$, ## $p<0.01$, # $p<0.05$, '#' represents comparison with CIS group.

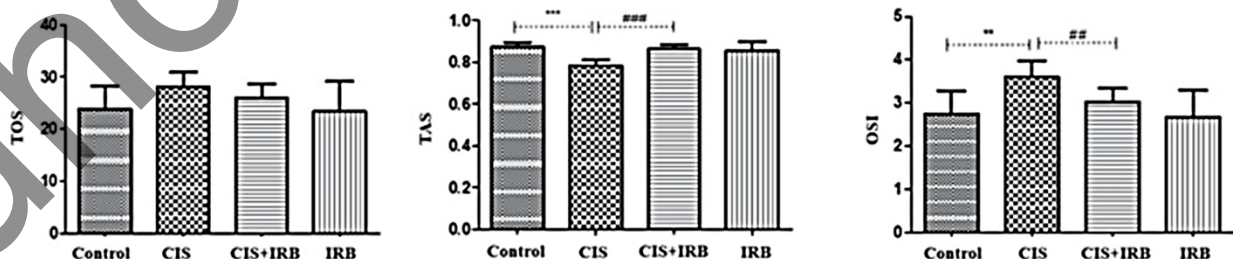


Figure 6: Oxidative stress parameters of liver tissues. Values are represented as means \pm SD. Comparison between groups and results of oxidative stress markers were assessed by one-way ANOVA test followed by post hoc Bonferroni multiple comparison test. *** $p<0.001$ ** $p<0.01$ * $p<0.05$, ‘*’ represents comparison with control group, ### $p<0.001$, ## $p<0.01$, # $p<0.05$, ‘#’ represents comparison with CIS group.

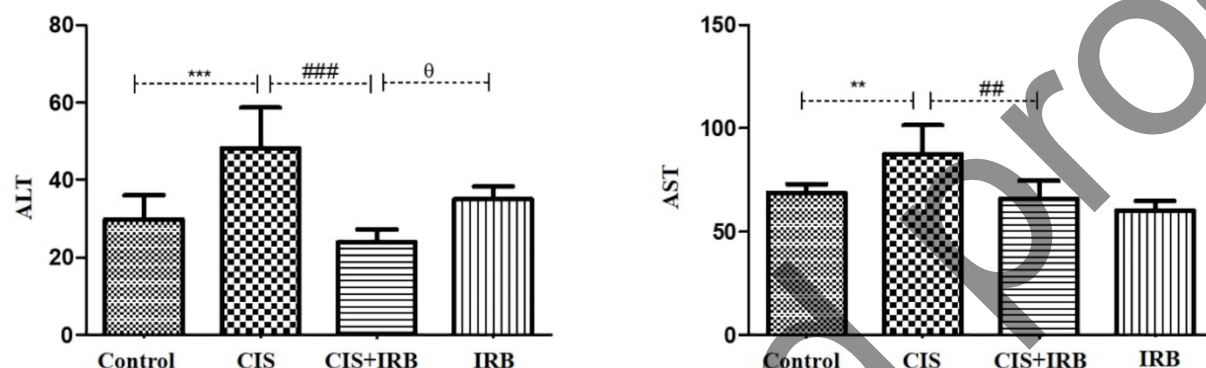


Figure 7: Evaluation of liver function parameters. Values are represented as means \pm SD. Comparison between groups and results of oxidative stress markers were assessed by one-way ANOVA test followed by post hoc Bonferroni multiple comparison test. *** $p<0.001$ ** $p<0.01$ * $p<0.05$, ‘*’ represents comparison with control group, ### $p<0.001$, ## $p<0.01$, # $p<0.05$, ‘#’ represents comparison with CIS group.